Biosynthesis of a novel ganoderic acid by expressing CYP genes from *Ganoderma lucidum* in *Saccharomyces cerevisiae*

Wen-Fang Wang[1], Han Xiao[1], and Jian-Jiang Zhong[1]

[1]Shanghai Jiao Tong University

April 28, 2020

Abstract

Heterologous production of 3-hydroxy-lanosta-8, 24-dien-26 oic acid (HLDOA) was recently achieved by expressing CYP5150L8 from *Ganoderma lucidum* in *Saccharomyces cerevisiae*, but post-modification of HLDOA remains unclear. In this study, another P450 from *G. lucidum*, CYP5139G1, was identified to be responsible for C-28 oxidation of HLDOA, resulting in the formation of a new ganoderic acid (GA) 3,28-dihydroxy-lanosta-8, 24-dien-26 oic acid (DHLDOA) by the engineered yeast, whose chemical structure was confirmed by LC-MS and NMR. In vitro enzymatic experiments confirmed the oxidation of HLDOA to DHLDOA by CYP5139G1. As the DHLDOA production was low (0.27 mg/L), to improve it, the strategy of adjusting the dosage of hygromycin and geneticin G418 to respectively manipulate the copy number of plasmid pRS425-Hyg-CYP5150L8-iGLCPR (harboring CYP5150L8, iGLCPR and hygromycin resistant gene hygR) and pRS426-KanMx-CYP5139G1 (harboring CYP5139G1 and G418 resistant gene KanMx) was adopted. Finally, 2.2 mg/L of DHLDOA was obtained, which was 8.2 fold of the control (without antibiotics addition). The work not only enriches the library of GAs and GA biosynthetic enzymes, but also helps to construct heterologous cell factories for other GA production as well as to elucidate the authentic GA biosynthetic pathway in *G. lucidum*.

1. INTRODUCTION

Ganoderic acids (GAs), a group of highly oxygenated lanostane-type triterpenoids, are well recognized as the primary ingredient of*Ganoderma lucidum* , a traditional famous medicinal basidiomycete, as they possess unique bioactivities such as anti-tumor and anti-metastasis effects (Bishop et al., 2015; Shiao, 2003; Wu et al., 2013; Xiao and Zhong, 2016; Zhong et al., 2009). The GAs exhibit a wide range of structural diversity, and up to now more than 150 kinds of GAs have been reported (Baby et al., 2015; Li et al., 2018; Liang et al., 2019). They were hypothesized to be derived from the key precursor lanosterol undergoing extensive oxidations catalyzed by cytochrome P450 enzymes (CYPs) (Chen et al., 2012; Xiao and Zhong, 2016). We reported its initial key enzyme - lanosterol C-26 oxidase CYP5150L8, which could convert lanosterol to 3-hydroxy-lanosta-8,24-dien-26-oic acid (HLDOA) in a heterologous host - *Saccharomyces cerevisiae* (Wang et al., 2018). However, it is yet difficult to biosynthesize other GAs in a heterologous host like yeast, because the subsequent biosynthetic steps from HLDOA to other GAs remain unknown.

Mining the catalytic enzymes involved in post-modification of HLDOA is critical to the heterologous synthesis of other GAs. Overall, 197 CYP genes have been annotated from analyses of the *G. lucidum* genome, some of which were supposed to participate in GA biosynthesis (Chen et al., 2012). Due to the chemical structure difference of various GAs and the catalytic behavior of CYPs, hydroxylation/oxidation of GA skeleton at the C-7, C-12, C-15, C-22 or C-23 position is likely to be achieved by CYPs. Recently, CYP512U6 was reported to be responsible for the hydroxylation of GA-DM and GA-TR at C-23 position (Yang et al., 2018). But, in their work, use of expensive substrates GA-DM and GA-TR was required to synthesize hainanic acid A and GA-Jc, which is not helpful to synthesize GAs from a cheap and simple carbon source such as glucose. Therefore, taking the HLDOA-producing yeast (Wang et al., 2018) as a starting platform to further mine

other key enzymes is considered as practical and critical for gradually elucidating the biosynthetic pathway of GAs as well as for their heterologous production.

In this work, we systematically screened candidate CYP genes by using the HLDOA producing yeast, and identified a functional *CYP5139G1* which could convert HLDOA to a new product. Then, the product was purified and its chemical structure was identified. Finally, we expressed both *CYP5150L8* and *CYP5139G1* by adopting a tunable expression strategy, and significantly enhanced the new GA production titer. The results will be helpful to further elucidating the synthetic pathway of GAs and constructing heterologous cell factories for efficient GAs production.

2. MATERIALS AND METHODS

2.1 Yeast cultivation

The strain *S. cerevisiae* YL-T3 (Wang et al., 2018) was grown in YPD medium (containing 10 g/L of yeast extract, 20 g/L of beef peptone, 20 g/L glucose). The recombinant yeast transformants were selected on SC-His-Leu-Ura (containing 20 g/L of glucose, 6.7 g/L of YNB, 0.65 g/L of Do-His-Leu-Ura3) plates at 30 °C (Dai et al., 2012), and these transformants were grown in SC-His-Leu-Ura liquid medium at 30 °C and 220 rpm

2.2 Construction of plasmids and engineered strains

Primers and plasmids used in this study are listed in Table S1 and Table S2, respectively. CYP5150L8 expression cassette was amplified with prime pair HXT7p-CYP5150L8-F/ FBA1t-CYP5150L8-R from plasmid pRS426-HXT7p-CYP5150L8-FBA1t (Wang et al., 2018). Plasmid pRS425-iGLCPR-Hygr (Lan et al., 2019) was linearized by *Pme* I (NEB, Beijing, China). The amplified CYP5150L8 fragment and linearized pRS425-iGLCPR-Hygr were ligated to produce plasmid pRS425-Hyg-CYP5150L8-iGLCPR according to the procedure described in SoSoo cloning kit (Tsingke, Beijing, China).

The G418-resistance gene *KanMX* was amplified from plasmid pUG6 (Guldener et al., 1996) with primer pair KanMX-F/KanMX-R (Table S1). A truncated *URA3* promoter was adopted to drive the transcription of*KanMX* (Bao et al., 2015). The B*amH* I linearized plasmid pRS426-HXT7p-FBA1t and *KanMX* expression cassette were assembled to produce plasmid pRS426-HXT7p-FBA1t-KanMX by DNA assembler (Shao et al., 2009). The P*me* I linearized plasmid pRS426-HXT7p-FBA1t-KanMX and CYP5139G1 expression cassette (amplified with primer pair HXT7p-CYP5139G1-F/FBA1t-CYP5139G1-R) was ligated to produce plasmid pRS426-KanMX-CYP5139G1 according to the procedure described in SoSoo cloning kit.

The plasmid pRS425-Hyg-CYP5150L8-iGLCPR and a series of CYP gene carrying plasmids (pRS426-CYPx), which we constructed previously (Wang et al., 2018), were transformed into *S. cerevisiae* YL-T3 to generate corresponding engineered yeast transformants (Table S3) using standard lithium acetate protocol (Gietz et al., 2007). Plasmid pRS425-Hyg-CYP5150L8-iGLCPR and plasmid pRS426 were also transformed into YL-T3 and served as a control. Plasmids pRS425-Hyg-CYP5150L8-iGLCPR and pRS426-KanMX-CYP5139G1 were transformed into YL-T3 to generate the strain HygL8-G418G1 (Table S3).

2.3 Fermentation, analyses of cell growth and product accumulation

For seed culture, strains were grown in SC-His-Leu-Ura at 30 °C and 220 rpm to an OD_{600} of 2-3. For shake-flask fermentation, the seeds were inoculated into 250 mL flasks containing 50 mL of YPD medium with appropriate concentrations of G418 and Hyg at an initial OD_{600} of 0.05 and then grew at 30 °C and 220 rpm. The fermentation data represented the means ± S.D. of three independent samples.

For detection of compound **A** , 15 mL of yeast culture was mixed with an equivalent volume of ethyl acetate and vortexed for 30 min. After centrifugation (12,000 g, 4 °C, 10 min), the supernatant was collected and evaporated (-0.1Mpa, 40 °C). Then, the dried product was re-dissolved in methanol for HPLC (Agilent, Waldbronn, Germany) analysis. Samples were assayed on an Agilent SB-C18 column (5 μm, 4.6 mm × 250 mm). Mobile phase A was 100% water, and mobile phase B contained methanol/acetic acid (100:0.1 v/v). A linear gradient for 80% to 100% B in 30 min at 1 ml/min was adopted.

2.4 *In vitro* enzymatic reactions

The yeast strains CPR-CYP5139G1 and CPR-EV (Table S3) were cultivated for microsome isolation. Microsomal isolation was performed as previously described (Wang et al., 2018). The enzymatic assay was conducted in a total volume of 500 μL of 90 mM Tris-HCl (pH 7.5) containing 500 μg microsomal protein and 2 mM NADPH; and 100 μM of a substrate - 3-hydroxy-lanosta-8,24-dien-26-ol (HLDO), 3-hydroxy-lanosta-8,24-dien-26-al (HLDA), or HLDOA was added, respectively. After incubation at 30 °C for 4 h, the product was extracted by ethyl acetate. The ethyl acetate layer was collected, evaporated, and redissolved in methanol for LC-MS analysis.

2.5 Purification of compound A

Compound **A** was extracted by 20 L ethyl acetate. The organic phase was collected by centrifugation (12,000 g, 4 °C, 10 min) and evaporated by a rotary evaporator (-0.1Mpa, 40 °C). About 50 ml of a brown oily liquid crude extract was finally obtained. Then, the crude extract was diluted three fold with methanol and separated by the preparative Agilent 1200 LC system (Waldbronn, Germany) equipped with a preparative Kromasil column (10 mm × 250 mm, Bohus, Sweden). Mobile phase A was 100% water and mobile phase B was methanol. A linear gradient of 80% B to 100% B in 30 min at 10 mL/min was chosen. Collected elutes from 22.4 to 24.4 min was stored at 4 °C overnight for precipitation. The solid as precipitated from the elutes was collected by centrifugation (12,000 g, 10 min), re-dissolved with methanol, and subjected to the preparative Agilent 1200 LC system equipped with a preparative ODS-BP C18 column (10 mm × 250 mm, Dalian, China). Mobile phase A was 100% water and mobile phase B was methanol. A linear gradient of 80% B to 100% B in 30 min at 2.5 mL/min was conducted. Elutes from 21.0 to 21.6 min was collected, and 2.4 mg of purified compound **A** was finally obtained.

2.6 Determination of plasmid copy number and gene expression level

Total DNA and RNA of the engineered yeast HygL8-G418G1 under different extraction conditions were collected and used for determining the plasmid copy number and the gene expression level, respectively. DNA was extracted by hydroxybenzene-chloroform-isoamyl alcohol (25:24:1) method. Firstly, cells were harvested by centrifugation (12,000 g, 5 min) and suspended with 500 μl PBS buffer. Added with a few glass beads and 500 μl phenol/chloroform/isoamyl alcohol (25:24:1), the cells were broken through the tissuelyser (JingXin, Shanghai, China), then centrifuged at 12,000 g, 10 min, 4 °C. The aqueous phase (top) was transferred to a new tube, added with 400 μl chloroform, and mixed gently. Then, it was centrifuged at 12,000 g, 10 min, 4 °C, and the supernatant was transferred to another new tube. It was added with 800 μl ethanol and mixed gently, kept at -20 °C for 2 h, then centrifuged at 12,000 g, 10 min, 4 °C. The resultant precipitation pellet was washed by 75% ethanol twice, and air-dried at 37 °C to evaporate the ethanol. Finally, the genome DNA was dissolved in 100 μl sterilized water for qPCR analysis. Total RNA was obtained by using yeast total RNA isolation kit (Sangon Biotech, Shanghai, China). The quantitative real-time polymerase chain reaction (qPCR) was carried out as previously reported (Lan et al., 2019) to determine the plasmid copy number and gene expression level. Primer pairs qCYP5150L8-F/qCYP5150L8-R, qCYP5139G1-F/qCYP5139G1-R, qiGLCPR-F/qiGLCPR-R and qERG2-F/qERG2-R, qTAF10-F/q-TAF10-R were designed for target genes and reference genes in qPCR reactions, respectively (Table S1). SYBR Green Real-Time PCR Master Mix (NEB, Beijing, China) on a qPCR apparatus (qTOWER3G touch, Analytikjena, Germany) was used for the analysis.

2.7 LC- MS and NMR analyses

LC-MS was carried out as previously reported (Wang et al., 2018). The NMR spectra of purified compound **A** were obtained by running 600 MHz Nuclear Magnetic (Avace III 600Hz, Karlsruhe, Germany) in DMSO solvent.

3. RESULTS

3.1 Identification of a CYP catalyzing HLDOA

Previously, from the *G. lucidum* genome, we narrowed down to 82 candidate genes which may be responsible for GA biosynthesis (Wang et al., 2018). In order to extend the biosynthetic step from HLDOA to a further GA, here we re-screened those genes by using the previously developed yeast chassis. Both plasmids pRS426-CYPx (Ura3 selection marker) and pRS425-CYP5150L8-iGLCPR (Leu selection marker) were co-transformed into *S. cerevisiae* YL-T3 to yield various engineered strains (Fig. 1a, Table S3). Considering that the biosynthetic genes of secondary metabolites may be arranged in cluster, we first examined whether the CYP genes located in the same gene cluster as CYP5150L8, i.e., CYP5150L6, CYP5150L9, CYP5150K5, CYP5150J5 and CYP5150J10, could catalyze HLDOA. The results showed that they could not catalyze, as no new peak appeared (Fig. 1b), suggesting that the GA biosynthetic genes might not be simply clustered together.

From the fermentation samples of the CYP5139G1 and CYP5150L8 (L8) co-overexpressed strain, generation of a new peak in the HPLC chromatogram was found (Fig. 1c). The peak with retention time (Rt) of 17.5 min could not be detected in either CYP5150L8 or CYP5139G1 single gene expressed strain, not to mention in the control with void plasmid.

By LC-MS analysis, compound **A** was detected with m/z at 455.3513 and 437.3410 (Fig. 1d), which was consistent with the molecular weight of $[C_{30}H_{48}O_4\text{-}H_2O+H]^+$455.3525 and $[C_{30}H_{48}O_4\text{-}2H_2O+H]^+$437.3420, respectively. Compared to HLDOA ($C_{30}H_{48}O_3$), it was supposed that hydroxylation of HLDOA to compound **A** might have occurred, and cyp5139G1 was considered responsible for the hydroxylation of HLDOA.

3.2 Purification and identification of compound A

Succeeding to the above finding, we used the Agilent semi-preparative HPLC equipped with a preparative column (Kromasil) for the initial purification of the target compound (compound **A**). An eluent tube was collected every 0.2˜0.3 min, and the preparative liquid chromatogram was shown in Fig. 2a. The eluent collected at 22.4, 23.1, 24.1 and 26.3 min (Fig. 2a inset) was analyzed by analytical HPLC, and it was found that the fractions around Rt 22.4˜24.1 mainly contained compound **A** , while the fraction at Rt 26.3 mainly had interference compounds (Fig. 2b). The crude product was obtained by combining those fractions between 22.4˜24.1 min of Rt. Then, the collection was further subjected to Agilent semi-preparative HPLC equipped with a preparative Hypesil ODS-BP column. The eluent fractions between 20.2˜22.5 min were again collected every 0.2 min (Fig. 2c), and detected by analytical HPLC. It was seen that the fractions at Rt 20.2 min or 22.5 min are impurities (Fig. 2d). The eluent around Rt 21.2 min was collected. After the removal of methanol and water by rotary evaporation and freeze-drying, finally 2.4 mg purified compound**A** was obtained.

To determine the chemical structure of compound **A** , we did various NMR analyses besides LC-MS/MS. The ^{1}H-NMR and^{13}C-NMR spectra of compound **A** (Table 1, Fig. S2 and S3) indicated six methyl groups and one hydroxymethyl group, while the substrate HLDOA has seven methyl groups and no hydroxymethyl group. The fact showed that compound **A** was a hydroxylated product of a methyl group of HLDOA. Comparing these spectroscopic data with those of HLDOA (Wang et al., 2018), the shift values of C-28 and C-29, both of which are connected to C-4 carbon atom, are significantly different (Table 1), suggesting that one of the two methyl groups was hydroxylated. The NOESY (nuclear overhauser effect spectroscopy) spectrum data of compound **A** revealed that 3-β-OH interacted with 29-β-CH_3, but did not with 28-CH_2OH (Fig. 3a), indicating that the orientation of hydroxylated methyl group and 3-β-OH was different, that is, the hydroxylation reaction occurred at the 28-α-CH_3 of HLDOA. Integrated with the data of distortionless enhancement by polarization transfer (DEPT) spectra, heteronuclear multiple-bond correlation (HMBC), heteronuclear single quantum coherence (HSQC) and homonuclear correlation spectroscopy (COSY) (Fig. S4, S5, S6 and S7), the structure of compound **A** was finally determined to be 3,28-dihydroxy-lanosta-8, 24-dien-26-oic acid (DHLDOA) (Fig. 3b), whose structure has not yet been reported.

3.3 Verification of CYP5139G1 catalytic function by *in vitro* enzymatic reaction

To verify the C-28 oxidase activity of CYP5139G1, we used *in vitro* microsome reaction system as previously

(Wang et al., 2018). The microsomal fractions from yeast YL-T3 expressing CYP5139G1 (strain CPR-CYP5139G1, Table S3) were incubated with HLDOA in the presence of NADPH at 30°C for 2 h. LC-MS analysis of the reaction mixture revealed that the CYP5139G1 containing microsome produced a new peak with the same retention time as the purified compound **A** (DHLDOA). No reaction was observed in boiled microsome sample or in that with void plasmid (strain CPR-EV, Table S3) (Fig. 4a). The LC-MS fragmentation pattern of the new peak included fragments with m/z ratios of 437 $[M\text{-}2H_2O+H]^+$ and 455 $[M\text{-}H_2O+H]^+$, which were consistent with those of the purified DHLDOA (Fig. 4b). The results demonstrated that CYP5139G1 catalyzed the conversion of HLDOA to DHLDOA.

We did not observe any hydroxylated products of HLDO and HLDA in the strain CYP5150L8-P45 (Table S3). In order to understand whether CYP5139G1 could catalyze C-28 hydroxylation of HLDOA derivatives - HLDO and HLDA, we used CYP5139G1 containing microsome incubated with HLDO and HLDA, respectively. As a result, no HLDO or HLDA oxidation was observed compared with the boiled CYP5139G1 harboring microsome and the void plasmid control (data not shown). Those evidences indicated CYP5139G1 had a strong substrate specificity to HLDOA.

Taking all the above facts together, we could conclude that CYP5139G1 was a HLDOA C-28 hydroxylase. By introducing CYP5139G1 into the yeast chassis, the reconstructed GA biosynthetic pathway from glucose was extended from HLDOA to DHLDOA. Here, both a novel GA and a new hydroxylase were found (Fig. 5).

3.4 Improving the DHLDOA biosynthesis in yeast with a dual tunable plasmid system

To explore whether the production of DHLDOA can be improved via regulating the CYP5150L8 and CYP5139G1 gene expression levels, here, two plasmids pRS425-Hyg-CYP5150L8-iGLCPR and pRS426-KanMX-CYP5139G1, which could be regulated by Hyg and G418, respectively, were co-transformed into *S. cerevisiae* YL-T3 to generate the strain HygL8-G418G1. By testing different combinations of Hyg (0, 100, 200, 300 mg/L) and G418 (0, 100, 300, 500, 700 mg/L) concentrations, we observed that DHLDOA had the highest titer when the Hyg and G418 concentration was at 100 mg/L and 300 mg/L, respectively (Fig. 6b, Fig. S1). To better understand this phenomenon, we further analyzed the production of HLDOA and DHLDOA, copy number of plasmids as well as transcription levels of CYP5150L8 and CYP5139G1 in the HygL8-G418G1 strain (Fig. 6). For the HygL8-G418G1 strain, the control without addition of antibiotics (H0G0) was set; fermentations with Hyg concentration at 100 mg/L while G418 concentration at 0, 100, 300, and 500 mg/L (H100G0, H100G100, H100G300, H100G500, respectively) were done; and those with G418 concentration at 300 mg/L while Hyg at 0, 100, and 200 mg/L (H0G300, H100G300, H200G300, respectively) were also conducted. It was found that in the control (H0G0), the production of HLDOA and DHLDOA was relatively low (4.62 mg/L and 0.27 mg/L, respectively). When 100 mg Hyg was added without G418 (H100G0), the DHLDOA titer decreased to 0.19 mg/L, although the accumulation of HLDOA increased to 14.43 mg/L (Fig. 6b). By comparing the copy number change of pRS425-Hyg-CYP5150L8-iGLCPR and pRS426-KanMX-CYP5139G1 plasmids between strains at H0G0 and H100G0, it was seen that with the addition of Hyg, the copy number of pRS425-Hyg-CYP5150L8-iGLCPR increased by 28 times and the transcription level of CYP5150L8 increased by 13.6 times; in contrast, the copy number of the plasmid pRS426-KanMX-CYP5139G1 and the transcription level of CYP5139G1 were low due to no addition of G418 (H0G0, H100G0) (Fig. 6c, 6d).

Under 100 mg/L of Hyg, with a higher addition of G418 (H100G0, H100G100, H100G300, H100G500), both the copy number of the plasmid pRS426-KanMX-CYP5139G1 and the transcription level of CYP5139G1 were increased by about 7˜10 times compared to H0G0. However, interestingly, compared with H100G0, although Hyg concentration was the same, with more addition of G418 (H100G100, H100G300, H100G500), the copy number of the plasmid pRS425-Hyg-CYP5150L8-iGLCPR decreased significantly (Fig. 6c). The results implied that the copy number of the two plasmids regulated by Hyg and G418 was not completely independent, which coincided with previous reports [32, 34]. A similar trend was seen in the transcription levels of CYP5150L8 and CYP5139G1 genes located in pRS425-Hyg-CYP5150L8-iGLCPR and pRS426-KanMX-CYP5139G1, respectively (Fig. 6d).

Under 300 mg/L of G418, the copy number of pRS426-KanMX-CYP5139G1 plasmid and the transcription level of CYP5130G1 were significantly increased (approximately 6-10 times) compared to that of H0G0. In addition, with the increase of Hyg (H0G300, H100G300, H200G300), the copy number of pRS425-Hyg-CYP5150L8-iGLCPR and the transcription level of CYP5150L8 also increased (Fig. 6c, 6d). Although the CYP5139G1 transcription level at H0G300 was 5.5 fold that of H0G0, due to the low copy number of pRS425-Hyg-CYP5150L8-iGLCPR plasmid and low transcription level of CYP5150L8, the production of HLDOA was low (3.1 mg/L), and the final DHLDOA titer was also very limited (0.48 mg/L). In the case of more pRS425-Hyg-CYP5150L8-iGLCPR plasmids and higher CYP5150L8 transcription levels at H200G300 vs. H100G300, the production of HLDOA and DHLDOA was 17.5 mg/L and 0.84 mg/L, respectively, which was almost 90% and 40% of the HLDOA and DHLDOA produced at H100G300, respectively, i.e., 17.5 *vs.* 21.8 mg/L; and 0.84 *vs.* 2.2 mg/L (Fig. 6). It seems that excessive expression of CYP5150L8 not only reduced the production of HLDOA, but also greatly reduced the production of DHLDOA. All the above results indicated that by manipulating antibiotics concentrations, both the plasmid copy number and the target gene transcription level could be adjusted; and both the gene expression level and their balanced expression were important. A suitable enhancement of CYP5150L8 and CYP5139G1 expression levels could improve the DHLDOA accumulation.

4. DISCUSSION

The present work showed a successful extension of the GA biosynthesis step by expressing a newly identified functional CYP5139G1 from *G. lucidum* in *S. cerevisiae* . Such work is certainly important to unveil the mystery of the GA post-modifications in *G. lucidum* . It is also critical to synthesize GAs in yeast chassis by synthetic biology. Our work of mining enzymes involved in GA biosynthesis and pathway reconstruction in *S. cerevisiae* has proved the feasibility of integrating gene mining with synthetic biology to produce GAs from the simple sugar glucose. Interesting, although there have been over 150 GAs reported from *G. lucidum* (Baby et al., 2015), the DHLDOA biosynthesized here was a new one. This may be because DHLDOA was quickly converted into the downstream GAs, failing to accumulate in *G. lucidum* . In another aspect, in the yeast cells, DHLDOA was accumulated due to the lack of subsequent enzymes that can catalyze DHLDOA. The work demonstrated that synthetic biology approach could not only produce known GAs, but also synthesized unnatural new GAs.

Generally, with the extension of biosynthetic steps, the end metabolite accumulation will dramatically decrease, which is a great challenge to natural product production by synthetic biology approach (Cravens et al., 2019). To increase the product titer is critical to determine its chemical structure with sufficient amount and high purity as well as to characterize the function of related enzyme(s). Up to now, many metabolic engineering strategies have been applied to improve the yield of target products, such as copy number engineering, promoter engineering, pathway enzyme engineering, co-factor engineering, and so on (Lian et al., 2018). Regulation of gene expression levels by adjusting plasmid copy number is a convenient and efficient approach to achieve a high accumulation of target natural products (Lan et al., 2019; Lian et al., 2016). Similar to a recent study (Lan et al., 2019), we used a dual tunable plasmid system to optimize the balanced expression of CYP5150L8 and CYP5139G1.

It can be observed that the copy number of the plasmid pRS426-KanMX-CYP5139G1 at H100G500 was more than that at H100G300, but the transcription level of CYP5139G1 did not increase (Fig. 6c, 6d), suggesting that the expression of the corresponding gene did not continue to increase with the increasing copy number when it exceeded a certain level. This may be due to that not only the copy number but also the transcription efficiency could affect the gene expression (Liu et al., 2020; Sha et al., 2013; Zhang et al., 2018). In addition, with the addition of the Hyg and G418, the cell growth was impaired (Fig. 6a). This may be due to 1) the toxicity of antibiotics (Balibar et al., 2016), 2) metabolic burden caused by high plasmid copy number and high level of foreign gene expression (Fig. 6c, 6d) on the cells (Hasunuma et al., 2015; Lan et al., 2019; Z. Liu et al., 2013), and/or 3) toxicity of the synthesized product (Qiao et al., 2019; Zhu et al., 2018). The problems of metabolic burden and product toxicity may be also the reason why the DHLDOA production decreased with the increased copy number of pRS426-KanMX-CYP5139G1 (Fig. 6b).

It was worth noting that by adopting the dual tunable plasmid system to adjust the ratio of CYP5139G1 to CYP5150L8 expressions, the DHLDOA production reached a maximum value of 2.2 mg/L at H100G300. In another aspect, at H0G300, the production of DHLDOA was not so high (0.5 mg/L), which may be due to insufficient supply of the substrate HLDOA. The results showed that the gene copy number adjustment was effective but had its limitation. Taking strategies including engineering at the mRNA level (Curran et al., 2013; Du et al., 2012), engineering at the protein level (Forman et al., 2018; Ignea et al., 2018), modifying suitable chassis cells or compartmentalization to accommodate the heterologous enzymes and so on (Cravens et al., 2019; Lian et al., 2018) may further improve the catalytic efficiency of CYP5139G1. In addition, considering the effect of CPR on CYP activity (Sugishima et al., 2014), and the mutual influence of multiple CYPs (Bassard et al., 2012; Xiao et al., 2019), pairing novel CPR, individually regulating the relative levels of CPR and CYPs and constructing efficient metabolon (multi-CYPs and CPR complex) (Gou et al., 2018; Laursen et al., 2016; S. Z. Wang et al., 2017), these measures may have the potential to achieve high catalytic efficiency for sequence reactions and to improve DHLDOA production.

In summary, here we succeeded in extending the GA biosynthetic step from HLDOA into producing a new GA, DHLDOA, by expressing CYP5139G1 from*G. lucidum* in the HLDOA producing *S. cerevisiae* . The DHLDOA production titer was significantly enhanced by modulating plasmid copy numbers. The study will be helpful to future extension of GA synthetic pathway, and it also helps to elucidate the authentic GA synthetic pathway in *G. lucidum,* as recently demonstrated by combining such work (Wang et al., 2018) with CRISPR/Cas9 based knocking-out of the gene CYP5150L8 (Wang et al., 2020). The study also laid a good foundation for future efficient biomanufacturing of various GAs using the established yeast chassis.

Acknowledgments

This work was supported by the National Key R&D Program of China (Nos. 2018YFA0900600, 2018YFA0901904, 2019YFA0904803), the National Natural Science Foundation of China (Nos. 31971344, 31770037), and Shanghai Municipal Natural Science Foundation (Nos. 17ZR1448900 and 18ZR1420300). We thank Prof. Meng Wang (Tianjin Institute of Industrial Biotechnology, Chinese Academy of Sciences, Tianjin) and Ms. Bo-Na Dai of Instrumental Analysis Center of SJTU for their helpful discussion on chemical structure determination of DHLDOA. We thank Ms. Ting-Ting Liu of our laboratory for her assistance in fermentation experiments.

Author contributions

J.J.Z. conceived the study, W.F.W., H.X. and J.J.Z. designed the experiments. W.F.W. performed experiments. W.F.W., H.X. and J.J.Z. analyzed experimental data. W.F.W. prepared the draft, H.X. gave advice on the manuscript, and J.J.Z. finalized the MS.

Additional Information

Additional supporting information may be found in the online version of this article at the publisher's web-site.

Conflict of Interests

The authors declare that there is no conflict of interests.

Reference

Baby, S., Johnson, A. J., & Govindan, B. (2015). Secondary metabolites from *Ganoderma* . *Phytochemistry, 114* , 66-101.

Balibar, C. J., & Roemer, T. (2016). Yeast: a microbe with macro-implications to antimicrobial drug discovery. *Briefings in Functional Genomics, 15* (2), 147-154.

Bao, Z., Xiao, H., Liang, J., Zhang, L., Xiong, X., Sun, N., . . . Zhao, H. (2015). Homology-integrated CRISPR-Cas (HI-CRISPR) system for one-step multigene disruption in *Saccharomyces cerevisiae* .*ACS Synthetic Biology, 4* (5), 585-594.

Bassard, J. E., Richert, L., Geerinck, J., Renault, H., Duval, F., Ullmann, P., . . . Werck-Reichhart, D. (2012). Protein-protein and protein-membrane associations in the lignin pathway. *Plant Cell, 24* (11), 4465-4482.

Bishop, K. S., Kao, C. H., Xu, Y., Glucina, M. P., Paterson, R. R., & Ferguson, L. R. (2015). From 2000 years of *Ganoderma lucidum* to recent developments in nutraceuticals. *Phytochemistry, 114* , 56-65.

Chen, S., Xu, J., Liu, C., Zhu, Y., Nelson, D. R., Zhou, S., . . . Sun, C. (2012). Genome sequence of the model medicinal mushroom*Ganoderma lucidum* . *Nature Communications, 3* , 913-921.

Cravens, A., Payne, J., & Smolke, C. D. (2019). Synthetic biology strategies for microbial biosynthesis of plant natural products.*Nature Communications, 10* (1), 2142-2154.

Curran, K. A., Karim, A. S., Gupta, A., & Alper, H. S. (2013). Use of expression-enhancing terminators in *Saccharomyces cerevisiae* to increase mRNA half-life and improve gene expression control for metabolic engineering applications. *Metabolic Engineering, 19* , 88-97.

Dai, Z., Liu, Y., Huang, L., & Zhang, X. (2012). Production of miltiradiene by metabolically engineered *Saccharomyces cerevisiae* . *Biotechnology and Bioengineering, 109* (11), 2845-2853.

Du, J., Yuan, Y., Si, T., Lian, J., & Zhao, H. (2012). Customized optimization of metabolic pathways by combinatorial transcriptional engineering. *Nucleic Acids Research, 40* (18), e142.

Forman, V., Bjerg-Jensen, N., Dyekjaer, J. D., Moller, B. L., & Pateraki, I. (2018). Engineering of CYP76AH15 can improve activity and specificity towards forskolin biosynthesis in yeast. *Microbial Cell Factories, 17* (1), 181-197.

Gietz, R. D., & Schiestl, R. H. (2007). High-efficiency yeast transformation using the LiAc/SS carrier DNA/PEG method. *Nature Protocols, 2* (1), 31-34.

Gou, M., Ran, X., Martin, D. W., & Liu, C. J. (2018). The scaffold proteins of lignin biosynthetic cytochrome P450 enzymes. *Nature Plants, 4* (5), 299-310.

Guldener, U., Heck, S., Fielder, T., Beinhauer, J., & Hegemann, J. H. (1996). A new efficient gene disruption cassette for repeated use in budding yeast. *Nucleic Acids Research, 24* (13), 2519-2524.

Hasunuma, T., Ishii, J., & Kondo, A. (2015). Rational design and evolutional fine tuning of *Saccharomyces cerevisiae* for biomass breakdown. *Current Opinion in Chemical Biology, 29* , 1-9.

Ignea, C., Pontini, M., Motawia, M. S., Maffei, M. E., Makris, A. M., & Kampranis, S. C. (2018). Synthesis of 11-carbon terpenoids in yeast using protein and metabolic engineering. *Nature Chemical Biology, 14* (12), 1090-1098.

Lan, X., Yuan, W., Wang, M., & Xiao, H. (2019). Efficient biosynthesis of antitumor ganoderic acid HLDOA using a dual tunable system for optimizing the expression of CYP5150L8 and a *Ganoderma* P450 reductase. *Biotechnology and Bioengineering, 116* (12), 3301-3311.

Laursen, T., Borch, J., Knudsen, C., Bavishi, K., Torta, F., Martens, H. J., . . . Bassard, J. E. (2016). Characterization of a dynamic metabolon producing the defense compound dhurrin in sorghum. *Science, 354* (6314), 890-893.

Li, X. M., Xie Y. Z., & Yang, B. B. (2018). Characterizing novel anti-oncogenic triterpenoids from ganoderma. *Cell Cycle, 17* (5), 527-528.

Lian, J., Jin, R., & Zhao, H. (2016). Construction of plasmids with tunable copy numbers in *Saccharomyces cerevisiae* and their applications in pathway optimization and multiplex genome integration.*Biotechnology and Bioengineering, 113* (11), 2462-2473.

Lian, J., Mishra, S., & Zhao, H. (2018). Recent advances in metabolic engineering of *Saccharomyces cerevisiae* : New tools and their applications. *Metabolic Engineering, 50* , 85-108.

Liang, C., Tian, D., Liu, Y., Li, H., Zhu, J., Li, M., . . . Xia, J. (2019). Review of the molecular mechanisms of *Ganoderma lucidum*triterpenoids: Ganoderic acids A, C2, D, F, DM, X and Y. *European Journal of Medicinal Chemistry, 174* , 130-141.

Liu, J., Han, Q., Cheng, Q., Chen, Y., Wang, R., Li, X., . . . Yan, D. (2020). Efficient expression of human lysozyme through the increased gene dosage and co-expression of transcription factor Hac1p in*Pichia pastoris* . *Current Microbiology*(10.1007/s00284-019-01872-9).

Liu, Z., Hou, J., Martinez, J. L., Petranovic, D., & Nielsen, J. (2013). Correlation of cell growth and heterologous protein production by *Saccharomyces cerevisiae* . *Applied Microbiology and Biotechnology, 97* (20), 8955-8962.

Qiao, J., Luo, Z., Cui, S., Zhao, H., Tang, Q., Mo, C., . . . Ding, Z. (2019). Modification of isoprene synthesis to enable production of curcurbitadienol synthesis in *Saccharomyces cerevisiae* .*Journal of Industrial Microbiology & Biotechnology, 46* (2), 147-157.

Sha, C., Yu, X. W., Li, F., & Xu, Y. (2013). Impact of gene dosage on the production of lipase from *Rhizopus chinensis* CCTCC M201021 in*Pichia pastoris* . *Applied Biochemistry and Biotechnology, 169* (4), 1160-1172.

Shao, Z., Zhao, H., & Zhao, H. (2009). DNA assembler, an in vivo genetic method for rapid construction of biochemical pathways.*Nucleic Acids Research, 37* (2), e16.

Shiao, M. S. (2003). Natural products of the medicinal fungus*Ganoderma lucidum* : occurrence, biological activities, and pharmacological functions. *Chemical Record, 3* (3), 172-180.

Sugishima, M., Sato, H., Higashimoto, Y., Harada, J., Wada, K., Fukuyama, K., & Noguchi, M. (2014). Structural basis for the electron transfer from an open form of NADPH-cytochrome P450 oxidoreductase to heme oxygenase. *Proceedings of the National Academy of Sciences of the United States of America, 111* (7), 2524-2529.

Wang, W. F., Xiao, H., & Zhong, J. J. (2018). Biosynthesis of a ganoderic acid in *Saccharomyces cerevisiae* by expressing a cytochrome P450 gene from *Ganoderma lucidum* . *Biotechnology and Bioengineering, 115* (7), 1842-1854.

Wang, S. Z., Zhang, Y. H., Ren, H., Wang, Y. L., Jiang, W., & Fang, B. S. (2017). Strategies and perspectives of assembling multi-enzyme systems. *Critical Reviews in Biotechnology, 37* (8), 1024-1037.

Wu, G. S., Guo, J. J., Bao, J. L., Li, X. W., Chen, X. P., Lu, J. J., & Wang, Y. T. (2013). Anti-cancer properties of triterpenoids isolated from *Ganoderma lucidum* - a review. *Expert Opinion on Investigational Drugs, 22* (8), 981-992.

Xiao, H., Zhang, Y., & Wang, M. (2019). Discovery and Engineering of Cytochrome P450s for Terpenoid Biosynthesis. *Trends in Biotechnology, 37* (6), 618-631.

Xiao, H., & Zhong, J. J. (2016). Production of Useful Terpenoids by Higher-Fungus Cell Factory and Synthetic Biology Approaches.*Trends in Biotechnology, 34* (3), 242-255.

Yang, C., Li, W., Li, C., Zhou, Z., Xiao, Y., & Yan, X. (2018). Metabolism of ganoderic acids by a *Ganoderma lucidum* cytochrome P450 and the 3-keto sterol reductase ERG27 from yeast.*Phytochemistry, 155* , 83-92.

Zhang, H., Yan, J. N., Zhang, H., Liu, T. Q., Xu, Y., Zhang, Y. Y., & Li, J. (2018). Effect of gpd box copy numbers in the gpdA promoter of*Aspergillus nidulans* on its transcription efficiency in*Aspergillus niger* . *FEMS Microbiology Letters, 365* (15).

Zhong, J. J., & Xiao, J. H. (2009). Secondary metabolites from higher fungi: discovery, bioactivity, and bioproduction. *Advances in Biochemical Engineering-Biotechnology, 113* , 79-150.

Zhu, M., Wang, C., Sun, W., Zhou, A., Wang, Y., Zhang, G., . . . Li, C. (2018). Boosting 11-oxo-beta-amyrin and glycyrrhetinic acid synthesis in*Saccharomyces cerevisiae* via pairing novel oxidation and reduction system

from legume plants. *Metabolic Engineering, 45* , 43-50.

Table 1. The ^{13}C-NMR and ^{1}H-NMR data of compound **A** .

C-position	^{13}C-NMR(ppm)	^{1}H-NMR (δppm, N.)
1	35.0	1.37 (m, 2H)
2	27.2	1.49 (m, 2H)
3	70.3	3.43 (m 1H)
4	42.0	-
5	41.9	1.38 (m 1H)
6	17.4	1.39 (m, 2H)-
7	27.7	1.88 (m, 2H)
8	133.6	-
9	134.4	-
10	36.3	-
11	22.0	1.99 (m, 2H)
12	30.6	1.64 (m, 2H)
13	44.1	-
14	48.4	-
15	30.5	1.12 (m, 2H)
16	25.6	2.00(m, 2H)
17	49.8	1.47 (m, 1H)
18	19.4	0.65 (s, 3H)
19	18.4	0.93 (s, 3H)
20	35.8	1.60 (m, 1H)
21	18.4	0.90 (s, 3H)
22	34.6	1.47 (m, 2H)-
23	25.0	2.04 (m, 2H)
24	142.1	6.63 (t, 1H)
25	127.4	-
26	168.9	-
27	12.2	1.71 (s, 3H)
28	64.4	3.08 (m, 2H)
29	12.5	0.55 (s, 3H)
30	24.1	0.83 (s, 3H)

Figure Legends

Figure 1 . Screening of CYPs involved with GA biosynthesis based on HLDOA. (a) The plasmid pRS425-iGlCPR-CYP5150L8 containing the iGlCPR and CYP5150L8 genes and the pRS426-CYPx plasmids (expressing different candidate CYP genes, respectively) were co-transformed into *S. cerevisiae* . (b) HPLC analyses of extracts from fermentation of *S. cerevisiae* transformants which co-expressed CYP5150L8 (L8) and CYP512U6 or other five CYP genes (CYP5150L6, CYP5150L9, CYP5150K5, CYP5150J5, CYP5150J10) which locate in the same cluster as CYP5150L8 in *G. lucidum* genome. Yeast transformant harboring plasmids pRS425-CYP5150L8-iGLCPR and void plasmid pRS426 served as control. (c) The transformant co-expressing CYP5150L8 and CYP5139G1 showed a new peak at 17.5 min. The expression of CYP5150L8 or CYP5139G1 alone had no new peak here. (d). High resolution MS spectra of compound **A**indicated in (c).

Figure 2 . Purification of compound **A** via Pre-HPLC. (a) Initial purification of Compound **A** via Pre-HPLC equipped with Kromasil column from which the fractions at different retention time are intercepted for detecting the compound **A** in different fractions. (b) HPLC analysis of different fractions (Rt 22.4, Rt 23.1, Rt 24.1, Rt 26.3) collected from first round purification indicated in (a). (c) Second round of purification of

compound **A** via Pre-HPLC equipped with ODS-BP C18 column. (d) HPLC detection of different fractions (Rt 20.2, Rt 21.2, Rt 22.5) separated by second round Pre-HPLC.

Figure 3 . The chemical structure of compound **A** . (a) NOESY spectra of compound **A** . Red circle represented the interaction between 29-CH3 and 3-β-OH. (b) Compound **A** was determined to be 3,28-Dihydroxy-lanosta-8,24-dien-26-oic acid (DHLDOA).

Figure 4 . *In vitro* microsomal reactions by CYP5139G1. (a) Compared to void plasmid and heated-CYP5139G1 control, microsomes containing CYP5139G1 generated a new peak with the same retention time as purified compound **A** (black line). (b) MS spectra of purified compound **A** (red line) and the product generated (red line) by microsome reaction with addition of HLDOA as substrate. For *in vitro* enzymatic assay, microsomes were prepared from YL-T3 containing void plasmid (control, blue line) or YL-T3 containing CYP5139G1 (red line). Heated-CYP5139G1 (gray line) represented that the CYP5139G1 containing microsomes were inactivated by heating at 80 °C.

Figure 5 . Reconstruction of GA biosynthetic pathway in *S. cereviae* . Single bold arrows represent one step reaction, while triple bold arrows represent multiple step reactions. Abbreviations: HMG-CoA, 3-hydroxy-3-methylglutaryl coenzyme A; IPP, isopentenyl pyrophosphate; DMAPP, dimethylallyl pyrophosphate; FPP, farnesyl diphosphate; HLDO, 3-hydroxy-lanosta-8,24-dien-26-ol; HLDA, 3-hydroxy-lanosta-8,24-dien-26-al; HLDOA, 3-hydroxy-lanosta-8,24-dien-26-oic acid; DHLDOA, 3,28-Dihydroxy-lanosta-8,24-dien-26-oic acid; HMGR, 3-hydroxy-3-methylglutaryl-CoA reductase; IDH, isopentenyl- diphosphate isomerase; ERG20, farnesyl diphosphate synthase; ERG9, squalene synthase; ERG1, squalene epoxidase; ERG7, lanosterol synthase.

Figure 6 . Modulation of CYP5150L8 and CYP5139G1 expression via plasmids with tunable copy numbers under different concentration combination of Hyg and G418. (a) Cell growth under different Hyg and G418 combinations including H0G0, H0G300, H100G0, H100G100, H100G300, H100G500, H200G300. (b) HLDOA and DHLDOA production after 5 days fermentation of strain HYGL8-G418G1 under the combination conditions mentioned above as (a). (c) Fold changes of pRS425-Hyg-CYP5150L8-iGLCPR and pRS426-KanMX-CYP5139G1 plasmid copy number under the conditions mentioned above (day 4 of fermentation). (d) CYP5150L8, CYP5139G1 relative expression in HYGL8-G418G1 strain with different conditions mentioned above in 4-day fermentation. The error bars represent the standard deviation of three biological replicates.

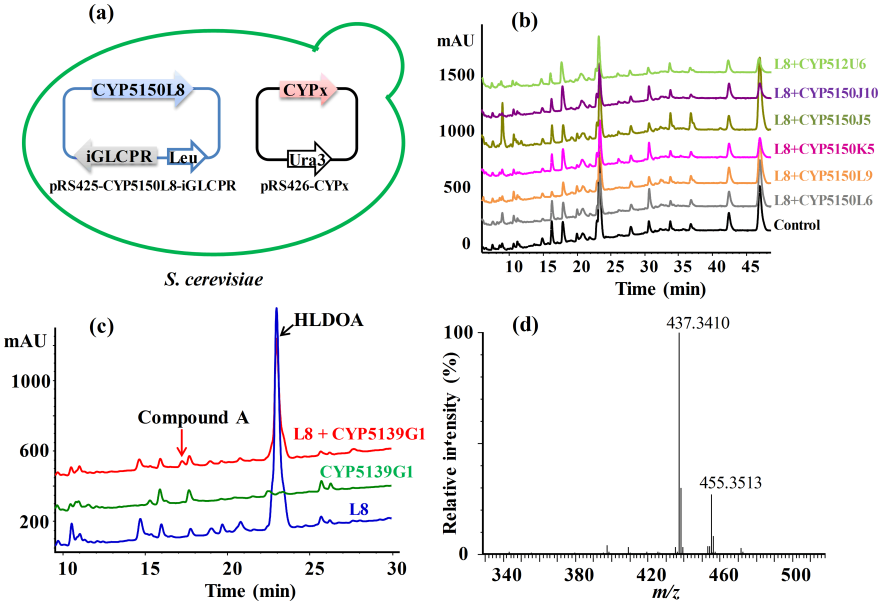

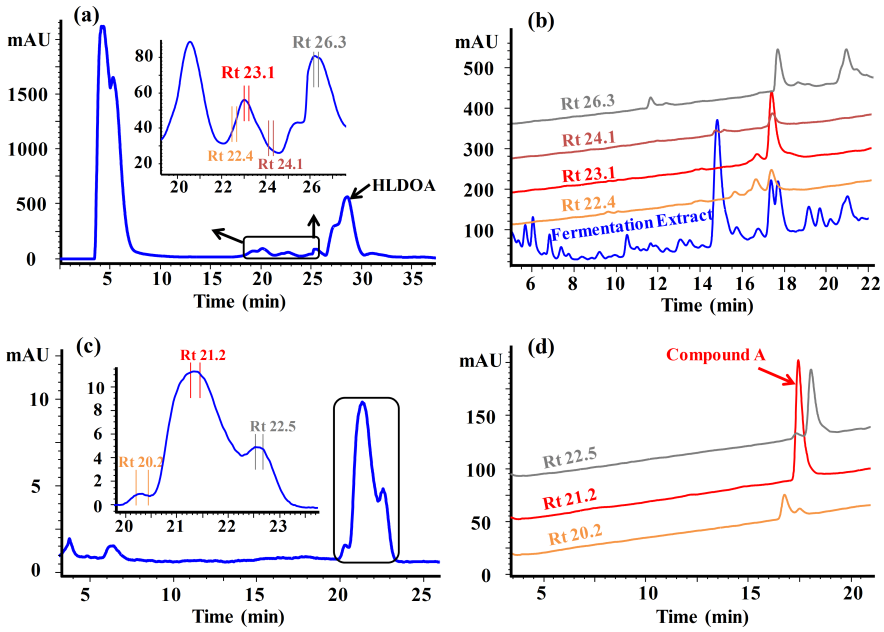

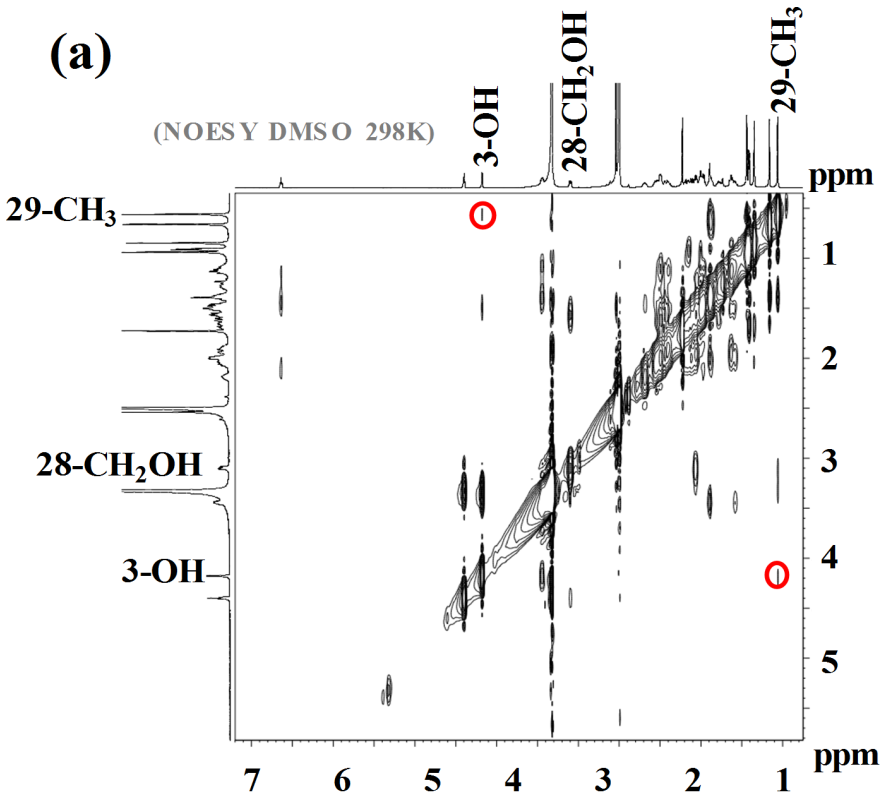

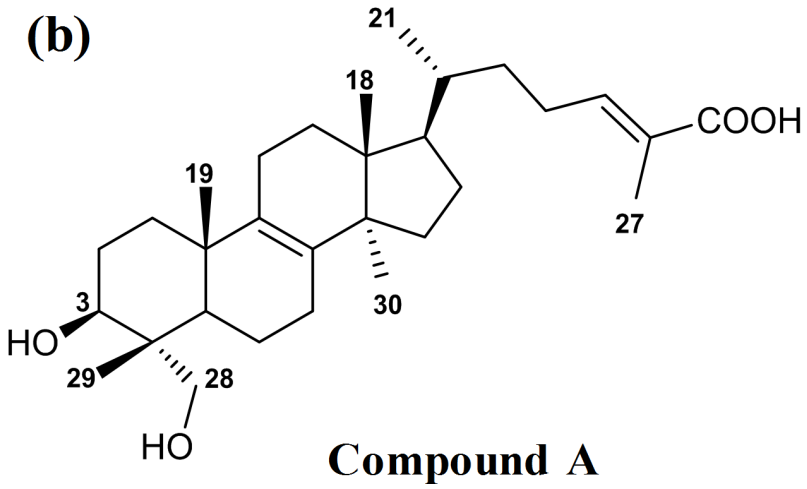

Compound A